CHEMICAL ENGINEERING TRANSACTIONS
VOL. 43, 2015
A publication of
AIDIC
The Italian Association
of Chemical Engineering
Online at www.aidic.it/cet
Chief Editors: Sauro Pierucci, Jiří J. Klemeš

ISBN 978-88-95608-34-1; **ISSN** 2283-9216
DOI: 10.3303/CET1543291

Synthesis of Hercynite at very Mild Condition

Matteo A.A. Daghetta*[a], Monica Dapiaggi[b], Lorenzo Pellegrino[a], Barbara Pastore[a], Lucia Pagliari[b], Carlo V. Mazzocchia[a]

[a] Department of Chemistry, Materials and Chemical Engineering “Giulio Natta”, Politecnico of Milano, Piazza Leonardo da Vinci 23, 20133 Milano
[b] Department of Earth Science “Ardito Desio”, Università degli Studi di Milano, Via Botticelli 23, 20133 Milano
matteoantonio.daghetta@gmail.com

Hercynite, Fe(II)Al_2O_4, is a double oxide with the spinel structure, found in rocks of various origin and composition. Due to its high hardness and thermal stability, it is exploited as an abrasive, in polishing/cutting tools and in refractories, such as in magnesia-hercynite refractory bricks.
Hercynite is not easily obtained as a monophasic material, and its synthesis is usually a highly energy demanding process. In fact, the two main methods of preparation, electro-fusion and traditional solid state route from the composing oxides, need very high temperatures (1450-1650 °C). To make matter more complex, the presence of Fe^{2+} ions requires any heating process to be performed under oxygen-free conditions. In this work a method for obtaining hercynite at 490-600 °C is reported. The synthesis involves a sol-gel reaction, followed by dehydration of the gel and calcination of the solid under nitrogen or nitrogen/hydrogen atmosphere. Different iron precursors have been tested. Hercynite percentage in the products ranged from 80 (wt) % to 100 (wt) %, depending on the experimental parameters. The products have been characterized by X-ray powder diffraction, thermogravimetric and elemental analyses, and scanning electron microscopy investigations.

1. Introduction

Hercynite is a greenish-to-dark-grey mineral with the spinel structure, that can be found in iron rich metamorphosed argillaceous sediments, as well as in mafic and ultramafic igneous rocks. It is characterized by a high hardness (Mohs scale 8.5) and an excellent thermal stability. These properties account for the main industrial uses of hercynite, which are the manufacturing of polishing or cutting tools (Milivoj et al., 2013) and magnesia-hercynite refractory bricks of cement rotary kilns (Zhang et al., 2012). In the field of refractories, magnesia-hercynite is the material of choice for substituting the traditional magnesia-chrome bricks, which show a deeply negative impact for Human health and Environment, due to the formation of carcinogenic Cr(VI) species during cement production. Different syntheses of hercynite are reported in literature. The two main preparation methods are electro-fusion and traditional solid-state reactions, both working in the temperature range between 1450 and 1800 °C (Chen et al., 2014). The presence of Fe^{2+} ions requires any heating process to be performed under oxygen-free condition. Chen et al. (2011) obtained pure hercynite by sintering alumina and mill scale (i.e. a mixture of FeO and Fe_2O_3), in the presence of carbon black under nitrogen atmosphere at 1550-1650 °C, while at lower temperatures (1450 °C) a mixture of alumina, magnetite and hematite was obtained. Ma et al. (2011) sintered hematite and alumina with various amounts of carbon black at a temperature above 1500 °C under nitrogen/oxygen atmosphere. As expected, lower oxygen partial pressures favor the obtainment of pure hercynite. A patent by Li et al. (2012) describes the synthesis of hercynite starting from ferric oxide, aluminum powder and activated aluminum oxide, under vacuum at 1200-1500 °C. Botta and co-workers (2002) reported the synthesis of hercynite from mechanochemically activated (Al + Fe_3O_4) mixture, heated at 1200 °C for 30 minutes under Ar atmosphere. The aim of this paper is to show that pure hercynite can be obtained in much milder conditions (in the temperature range 490-600 °C) by

Please cite this article as: Daghetta M., Dapiaggi M., Pellegrino L., Pastore B., Pagliari L., Mazzocchia C., 2015, Synthesis of hercynite at very mild condition, Chemical Engineering Transactions, 43, 1741-1746 DOI: 10.3303/CET1543291

means of a sol-gel approach: various conditions of reaction atmosphere and various iron precursors were tried, in order to optimize the synthesis process.

2. Materials and Methods

Sol-gel approach has been used to intimately mix iron and aluminum precursors. A summary of the syntheses conditions, together with the sample names, can be found in Table 1.

Table 1: Sample names and corresponding experimental conditions

Sample name	Precursor	T (°C)	Atmosphere
ESS1	$[Fe(NO_3)_3 \cdot 9H_2O]$, $[Al(NO_3)_3 \cdot 9H_2O]$	55	Air
CALC1	ESS1	490*	Air
CALCN1	ESS1	490*	Nitrogen
ESS2	$[NH_4]_3[Fe(C_2O_4)_3] \cdot 3H_2O$, $[Al(NO_3)_3 \cdot 9H_2O]$	55	Air
CALC2	ESS2	490*	Nitrogen
RED1	CALC1	600*	Nitrogen/hydrogen
REDN1	CALCN1	600*	Nitrogen/hydrogen
RED2	CALC2	600	Nitrogen/hydrogen
REDH2	RED2	1000	Nitrogen

* This temperature was used for the reaction, then a sample was heated up to 1000 °C under nitrogen atmosphere (air for CALC1) in order to favour the crystallization of the species.

2.1 Experimental details

X-ray powder diffraction. All powder diffraction patterns were collected on a Philips X'Pert MPD equipped with a graphite analyser, with a Cu Kalpha radiation, and 40 kV+40mA power. The data were collected between 10 and 70° 2theta, with a step size of 0.03° and a time per step of 2-3 s, depending on the sample.
All analytical reagents were purchased by Sigma-Aldrich and used as received.
ESS1. $[Fe(NO_3)_3 \cdot 9H_2O]$ (256,0 g, 0,634 mol) and $[Al(NO_3)_3 \cdot 9H_2O]$ (475,4 g, 1,267 mol) were dissolved in deionized water (0,600 L) and then $NH_4OH(aq)$ (33% v/v) was dropwise added under stirring until sudden gel formation (about 0,400 L, pH ~ 7). This gel was then dried at 55 °C for 8 hours.
CALC 1. ESS1 was manually grinded and the resulting powder was calcined in a fluidized bed reactor at 490 °C (heating ramp 8 °C/min) for 120 minutes in air flow ($8 \cdot 10^{-3}$ Nm^3s^{-1}), yielding 95 g of product
CALCN 1 ESS1 was washed with water (4x0,050 L) before the desiccation. Then the obtained solid was calcined in the same condition of CALC1 but using nitrogen instead of air
ESS2. $\{[NH_4]_3[Fe(C_2O_4)_3] \cdot 3H_2O\}$ (271,3 g, 0,634 mol) and $[Al(NO_3)_3 \cdot 9H_2O]$ (475,4 g, 1,267 mol) were dissolved in deionized water (0,600 L) was dropwise added under stirring until sudden gel formation. This gel was washed on a Buchner filter with water (4x0,050 L), then dried at 55 °C for 8 hours.
CALC 2 ESS 2 was manually grinded and the resulting powder was calcined in a fluidized bed reactor at 490 °C (heating ramp 8 °C/min) for 120 minutes in nitrogen flow ($8 \cdot 10^{-3}$ Nm^3s^{-1}), yielding 88 g of product.
RED 1, REDN 1, RED 2. A sample of CALC 1, CALCN 1 or CALC 2 respectively was heated up in a fluidized bed reactor under a nitrogen flow (10^{-4} Nm^3s^{-1}) to 600 °C (heating ramp 10 °C/min), then the atmosphere was switched to nitrogen/hydrogen 70:30 v/v maintaining the same flow rate and the same temperature for 0,5 hours. The solids were then kept in inert atmosphere by means of usual Schlenk techniques.
REDH 2. A sample of RED 2 was treated at 1000 °C under a nitrogen flow (10^{-4} Nm^3s^{-1}) for 0,5 hours.

3. Results and discussion

3.1 X-ray powder diffraction

ESS1 diffraction pattern shows only peaks attributable to NH_4NO_3 (figure 1a, bottom pattern), CALC1 remains amorphous at 490 °C (pattern not shown), and a crystallization occurs after heating up to 1000 °C, showing only peaks belonging to hematite and corundum (Figure 1a top pattern).

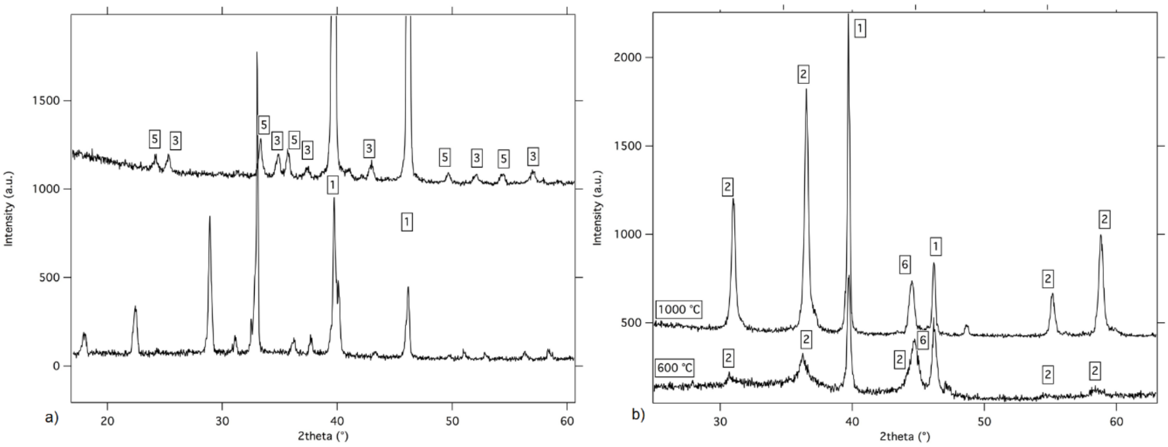

Figure 1: (a) sample ESS1 on the bottom (all peaks except those marked with 1 belong to ammonium nitrate), sample CALC1 on the top; (b) sample RED1 at 600 °C and 1000 °C. The number 1 in the figures refers to Pt sample holder peaks, the number 2 refers to hercynite peaks, the number 3 to corundum, the number 5 to hematite and the number 6 to iron.

A sample of CALC1 was then treated with nitrogen/hydrogen (70:30 v/v) at 600 °C (RED1, figure 1b, bottom pattern), leading to the complete reduction of hematite partially to α-iron and, by reaction with Al_2O_3, to hercynite. Heating it up to 1000 °C under nitrogen atmosphere results in crystallization increase, but no further reaction occurs (Figure 1b, top pattern).

ESS1, calcined in nitrogen flow at 490 °C, is completely amorphous (CALCN1, figure 2a, bottom pattern); crystallization only happen by heating at 1000 °C (figure 2a, top pattern), making evident the presence of corundum, hematite and magnetite. Finally, by exposing CALCN1 to a flow of nitrogen/hydrogen (70/30) a sample of pure hercynite is obtained (REDN 1, Figure 2b, bottom), whose identification is easier if the sample is heated at 1000 °C in nitrogen atmosphere (Figure 2b, top).

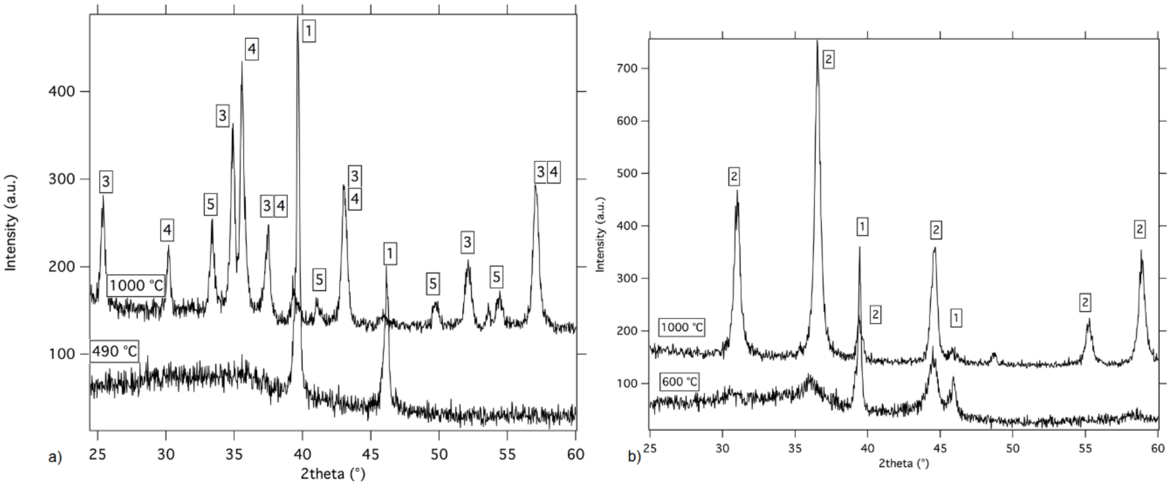

Figure 2: (a) Sample CALCN1, calcined at 490 °C (bottom pattern) and at 1000 °C (top pattern). (b) Sample REDN1, calcined at 600 °C (bottom pattern) and at 1000 °C (top pattern). The number 2 on the figures refers to hercynite peaks, the number 1 to the Pt sample holder, the number 3 refers to corundum peaks, the number 4 to magnetite peaks, the number 5 to hematite peaks.

ESS2 exhibits a different behavior. In fact, after calcination at 490 °C under nitrogen atmosphere, only hercynite is evident by XRPD (CALC2, Figure 3 bottom pattern). A treatment in nitrogen/hydrogen (70:30 v/v) at 600 °C (sample RED2), followed by heating at 1000 °C under nitrogen just increased the crystallization degree (sample REDH2, Figure 3 top pattern), but it is worth stressing that hercynite was formed yet at 490 °C in nitrogen.

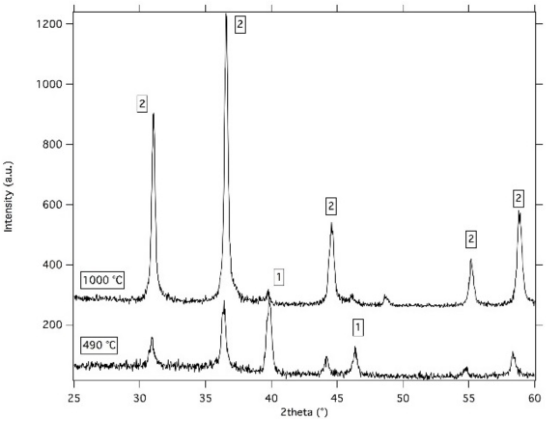

Figure 3: sample CALC2 (bottom pattern) and REDH2 (top pattern). The number 1 refers to Pt sample holder, the number 2 to hercynite peaks.

3.2 Scanning Electron Microscopy

A morphological investigation on a few significant samples has been conducted. Figure 4a shows a backscattering image of RED 1 sample. Here the contrast of the greyscale picture is due to different electron density of the constituent elements. Figure 4b instead is obtained with secondary electron emission, where contrast accounts for the morphology of the sample, being sensitive to its distance, along the z axis, from the detector. So the sample consists in an aggregate of less electron-rich particles, with isles of more electron-rich particles above. Matching these information with EDX spectra (Figure 4c) collected on two different portions, 1 and 2, allows to conclude that isles are constituted by iron, while the substrate can be considered as a mixture of aluminium oxide and an iron containing oxide, which we know to be hercynite from XRPD spectra.

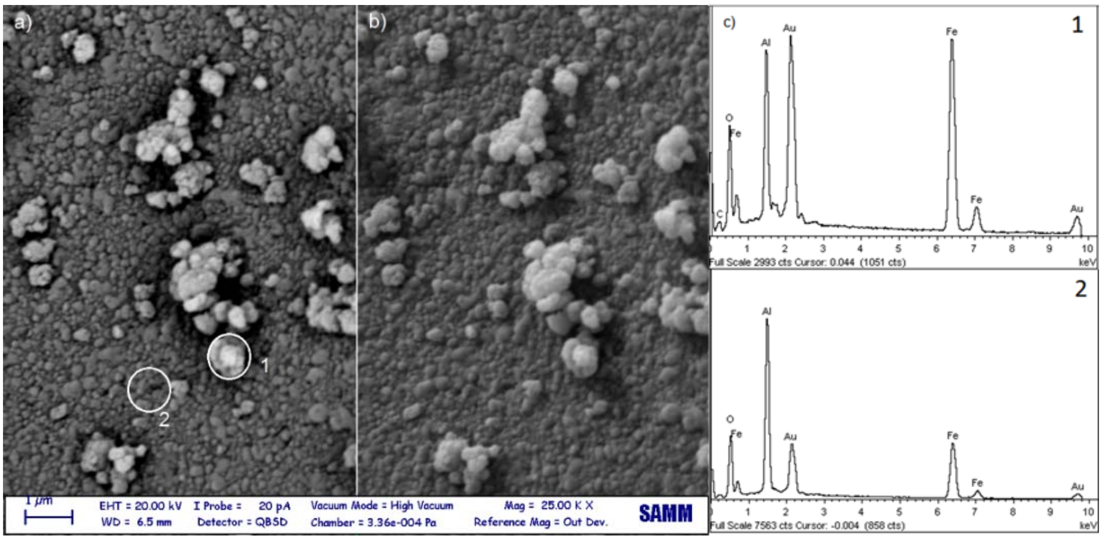

Figure 4: Micrography (25000x) of RED 1. a) backscattering image b) secondary electron emission image of the same region c) EDX spectra of portion 1 and 2 circled in figure 4a

CALC2 and RED 2 are shown in Figures 5a and 5b respectively. They are morphologically very similar to each other, and this confirms the fact that no further reaction occurs with exposing CALC 2 to hydrogen. Moreover, their morphology is very different from the one of RED 1 (Figure 4a-b). While the latter appeared as an aggregate of well defined particles, RED2 shows a smoother and more uniform surface, looking more as a single component solid.

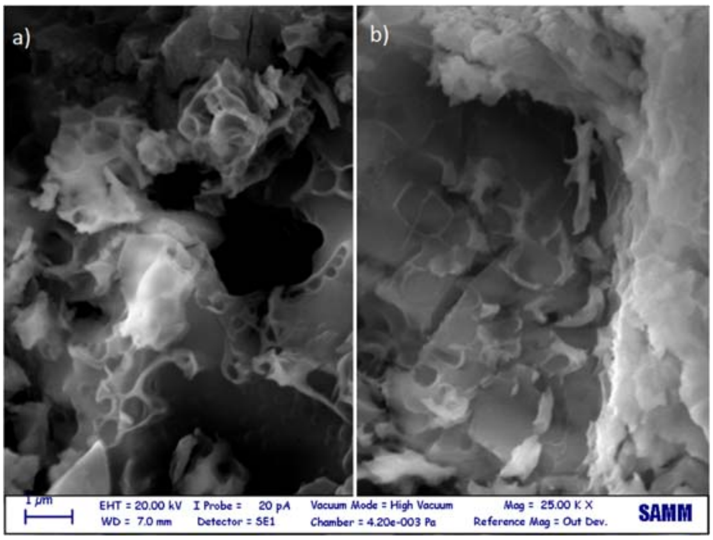

Figure 5: Backscattering micrography (25000x) of a) CALC2 b) RED 2

3.3 Thermogravimetric Analysis and Induced Coupled Plasma Mass Spectroscopy Analysis

Thermogravimetric analysis and Induced Coupled Plasma Mass Spectroscopy have been used in order to define the composition of RED 1. TGA, collected in air (10 °C/min 20-1000 °C), revealed just a weight gain of 2,963% between room temperature and 300 °C, while ICP are shown in Table 2.

Table 2: Calculated and experimental (ICP-MS) metal composition of RED 1

Formulation	Fe % (wt)	Al % (wt)
$FeAl_2O_4$	32,13	31,05
$Fe+Al_2O_3$	35,4	34,19
RED 1	32,4	32,1

We can consider the formulation of RED1 as an intermediate between two limit situation, pure hercynite and pure iron (35.4% w/w) over Al_2O_3, whose corresponding metal contents are given in Table 2. Otherwise, the weight gain of 2.963% below 300 °C can be assigned to the reaction $2\ Fe + 1.5\ O_2 \rightarrow Fe_2O_3$ as neither Al_2O_3 or hercynite are prone to oxidation (Pillay et al., 1960). If all the available iron (32.4 % wt) would oxidized to hematite the weight gain would be 13.92% so it can be deduced that only $2.963 / 13.92 \cdot 100 = 21.26$ % of the available iron is oxidized, that corresponds to 6,88% of metallic iron in the sample. The remaining 25.52 % of Fe is attributable to $FeAl_2O_4$ and considering the corresponding moles, which are the same of hercynite, it is possible to calculate that $FeAl_2O_4$ accounts for the 79.37 % of the sample. Finally the difference between the experimental amount of aluminium and the quantity attributed to hercynite results in a 14.05 % of Al_2O_3 which completes the formulation of the sample.

3.4 Discussion

Iron precursors and the atmosphere used during calcination demonstrated to have a prominent role in the resulting products. As expected, by using an oxidizing environment, Fe(III) oxide (hematite) is obtained, as well as starting from iron(III) nitrate or ammonium iron(III) oxalate. On the contrary, by using nitrogen, a difference in behaviour emerges. Starting from ESS1, upon calcination, a mixture of magnetite Fe_3O_4 and hematite is formed (CALCN 1), together with some aluminium oxide; on the other hand, in ESS2 iron(III) is reduced to iron (II), which reacts with aluminium species and yields to $FeAl_2O_4$.

Hercynite forms through the reaction between FeO and Al_2O_3 (Chen et al., 2011), so the reduction of iron(III) oxide to iron(II) oxide is the first step. In the case of ESS1, only a redox reaction with hydrogen may produce the necessary iron(II), while, in the case of ESS2, where hercynite forms in nitrogen atmosphere, the only possible reducing agent is $(C_2O_4)^{2-}$ which is oxidized to CO_2. During the addiction of ammonium hydroxide to the solution of ammonium iron(III) oxalate and aluminium nitrate, hydroxide anions partially substitute carboxylic oxygen atoms in the coordination sphere of iron. Instead of a complete decoordination of the dianion, a simple opening of the chelate is very likely to occur, leaving pending oxalates on iron(III) centres. In this condition the uncoordinated carboxylic atoms can easily bond to Al(III), obtaining a Fe-Al bridged species. If this occurred many times, the result is an extended network of Fe and Al centres linked by oxalates, as well as by oxo and hydroxo bridges. So, the formation of hercynite at low calcination temperatures, with respect to what reported in literature, can be attributed to the fact that iron and aluminium are very close one to each other. Oxalate has then a dual role, in reducing Fe(III) to Fe(II) and in bridging iron and aluminum.

It is also interesting to note the behaviour of the samples under reducing condition. CALC 1 results, after exposure to hydrogen 30% at 600 °C, in a mixture of hercynite, α-iron, and unreacted Al_2O_3. The presence of the last species, although unrevealed by XRPD, has been desumed from ICP and TG analyses. The reactions involve at least two solids and a gas, so it is quite easy to explain why this reaction is neither quantitative nor selective. It is known that magnetite, FeO and the defective $Fe_{1-x}O$ wustite are intermediate species in the reduction path from hematite to iron in hydrogen atmosphere (Pineau et al. 2006, 2007). It seems reasonable to state that in our condition most of hematite reacts with hydrogen forming FeO and this one reacts with aluminium oxide to give $FeAl_2O_4$. A part of FeO instead is not able to meet Al_2O_3. So this amount of FeO completes the reduction up to iron, aluminium oxide remaining the same.

On the contrary CALCN 1 selectively converted into hercynite, and this is probably due to the presence of some magnetite in the sample before the reduction step. This species is more easily reduced to FeO than Fe_2O_3 and so FeO is available to react with Al_2O_3 at lower temperature. The whole equilibrium is pushed towards the products and the reaction results quantitative and selective. Finally CALC 2, being yet constituted of hercynite, essentially does not react.

4. Conclusions

Sol-gel approach, followed by drying and calcination, has been used for hercynite synthesis. Differences between iron(III) nitrate and ammonium iron(III) oxalate have been evaluated. Hercynite has been obtained at lower temperature than reported in literature. An interpretation on the phenomenon is proposed.

References

Botta, P.M., Aglietti, E.F. & Porto López, J.M., 2002, Mechanochemical synthesis of hercynite. Materials Chemistry and Physics, 76(1), 104–109

Chen, J.H., Su J.D., Yan M.W., Yang S.L., Liu W.L., 2014, Two Methods of Synthesizing Hercynite. Applied Mechanics and Materials, 543-547, 3830–3833.

Chen, J.H., Yu L., Sun J., Li Y., Xue W., 2011, Synthesis of hercynite by reaction sintering. Journal of the European Ceramic Society, 31(3), 259–263.

Li D., Li H., Wang G., Wang L., Yuan Bo, 2012, Method for synthesizing hercynite. Available at: <http://www.google.com/patents/CN102583462A>, accessed 23-10- 2014.

Ma S., Li Y., Sun J., Wang Z., 2011, Synthesis of hercynites under N_2 atmosphere. Kuei Suan Jen Hsueh Pao/Journal of the Chinese Ceramic Society, 39(3), 424–429.

Milivoj K. B., Kebbede A., Sweeney S. M., Yosenick T. S., 2013, High strength, fine grained spinel for window applications, methods of manufacture therefore and articles comprising the same. Available at: http://www.google.com/patents/US8529827 [Accessed October 23, 2014].

Pillay, T.C.M., D'Entremont, J. & Chipman, J., 1960, Stability of Hercynite at High Temperatures. Journal of the American Ceramic Society, 43(11), 583–585.

Pineau, A., Kanari, N. & Gaballah, I., 2007, Kinetics of reduction of iron oxides by H_2: Part II. Low temperature reduction of magnetite. Thermochimica Acta, 456(2), 75–88.

Pineau, A., Kanari, N. & Gaballah, I., 2006, Kinetics of reduction of iron oxides by H_2: Part I: Low temperature reduction of hematite. Thermochimica Acta, 447(1), 89–100

Zhang, X., Yu, R. & Yu, X., 2012, Characteristics of hercynite and its application: In refractories. China's Refractories, 21(2), 17–22.